Available online at www.sciencedirect.com

SCIENCE DIRECT®

Coastal Engineering 51 (2004) 1067–1084

Coastal Engineering
An International Journal for Coastal, Harbour and Offshore Engineers

www.elsevier.com/locate/coastaleng

Wave momentum flux parameter: a descriptor for nearshore waves

Steven A. Hughes*

US Army Engineer Research and Development Center, Coastal and Hydraulics Laboratory, 3909 Halls Ferry Road, Vicksburg, MS 39180-6199, USA

Received 23 April 2003; received in revised form 29 June 2004; accepted 16 July 2004
Available online 7 October 2004

Abstract

A new parameter representing the maximum depth-integrated wave momentum flux occurring over a wave length is proposed for characterizing the wave contribution to nearshore coastal processes on beaches and at coastal structures. This parameter has units of force per unit crest width, and it characterizes flow kinematics in nonbreaking waves at a given depth better than other wave parameters that do not distinguish increased wave nonlinearity. The wave momentum flux parameter can be defined and estimated for periodic and nonperiodic (transient) waves. Thus, it has potential application for correlating to processes responding to different types of waves. This paper derives the wave momentum flux parameter for linear, extended linear, and solitary waves; and it presents an empirical formula estimating the parameter for nonlinear steady waves of permanent form. Guidance is suggested for application to irregular waves. It is anticipated that the wave momentum flux parameter may prove useful for developing improved semiempirical formulas to describe nearshore processes and wave/structure interactions such as wave runup, overtopping, reflection, transmission, and armor stability. Surf zone processes where waves break as plunging or spilling breakers may not benefit from use of the wave momentum flux parameter because the breaking processes effectively negates the advantage of characterizing the wave nonlinearity.
© 2004 Elsevier B.V. All rights reserved.

Keywords: Coastal structures; Iribarren number; Nonlinear waves; Solitary waves; Wave forces; Wave momentum flux; Wave parameters

1. Introduction

Coastal shore protection and navigation structures are designed to withstand waves up to an expected level (sometimes referred to as the "design wave"), and there are often multiple structure design criteria associated with the specified design wave. For example, a rubble-mound breakwater design must assure armor stability; and there may be specified values for maximum wave runup, allowable average rate of wave overtopping, and maximum height of transmitted waves. These design criteria are dependent on project functional requirements, so specified criteria may vary between projects.

* Tel.: +1 601 634 2026; fax: +1 601 634 3433.
E-mail address: steven.a.hughes@erdc.usace.army.mil.

0378-3839/$ - see front matter © 2004 Elsevier B.V. All rights reserved.
doi:10.1016/j.coastaleng.2004.07.025

The hydrodynamic interaction of waves with coastal structures is complex, and steady progress has been made toward understanding wave/structure interactions. However, some engineering aspects of coastal structure design are still not fully described by theory. Examples include rubble-mound armor stability, wave runup on permeable slopes, and wave overtopping of protective structures.

Engineers have established useful design guidance by augmenting theoretical reasoning with empirical coefficients determined from small-scale laboratory testing. The balance between theoretical and empirical contribution to coastal structure design guidance varies widely. For example, estimation of nonbreaking wave forces on vertical walls is largely theory with some empirical adjustments, whereas estimation of irregular wave runup on permeable structures is almost entirely empirical.

Waves are usually included in empirical design relationships by one or more wave parameters considered to be representative of the incident wave condition. Common regular and irregular wave parameters are listed Table 1. Sometimes, these wave parameters are combined to form dimensionless variables that may include relevant fluid parameters and other parameters such as those given in Table 1. This helps reduce the number of independent variables that need to be examined during laboratory testing. Table 2 lists the more common dimensionless wave parameters that are used in coastal structure design guidance.

Table 1
Common wave and fluid parameters

Regular wave parameters	
H—wave height	H_o—deepwater wave height
L—local wave length	L_o—deepwater wave length
T—wave period	k—wavenumber [$=2\pi/L$]
Irregular wave parameters	
H_{mo}—zeroth-moment wave height	H_s—significant wave height [$=H_{1/3}$]
H_{rms}—root-mean-squared wave height	$H_{10\%}$—10% of waves are higher
T_p—spectral peak wave period	T_m—mean wave period
L_p—wave length associated with T_p	L_{op}—deepwater wave length with T_p
L_m—wave length associated with T_m	L_{om}—deepwater wave length with T_m
Fluid and other parameters	
g—gravitational acceleration	ρ—fluid density
μ—coefficient of dynamic viscosity	ν—coefficient of kinematic viscosity
h—water depth	α—beach or structure slope

Table 2
Common dimensionless wave parameters

Parameter	Value
Relative depth	h/L; h/gT^2; kh
Relative wave height	H/h
Wave steepness	H/L; H/L_o; H/gT^2
Deepwater wave steepness	H_o/L_o; H_o/gT^2
Local Iribarren number, ξ	$\frac{\tan\alpha}{\sqrt{H/L}}$
Deepwater Iribarren number, ξ_o	$\frac{\tan\alpha}{\sqrt{H_o/L_o}}$ or $\frac{\tan\alpha}{\sqrt{H/L_o}}$

With the exception of relative wave height, H/h, the wave parameters listed in Table 2 strictly pertain to uniform, periodic waves of permanent form. It is customary to use first-order wave theory to calculate values for wave length. These dimensionless parameters are also used to characterize irregular waves trains by substituting wave heights, wave periods, and wave lengths representative of irregular waves, such as wave heights H_{mo}, H_{rms}, $H_{1/3}$, and $H_{10\%}$; wave periods T_p and T_m; and wave lengths L_p, L_{op}, L_m and L_{om}. (See list of symbols at end of paper for definitions of these irregular wave parameters.)

Correlations between dimensionless wave parameters and process responses observed in experiments form the basis for much coastal structure design guidance and some nearshore beach processes. Often, justification for using a particular wave parameter is not based on a physical argument, but simply because it produced the least scatter in the correlation. Only relative wave height, H/h, is applicable to solitary waves, although there are some definitions for solitary wave length which would allow use of the other wave parameters.

2. The Iribarren number

One parameter of proven usefulness for wave processes on beaches and at coastal structures is the

Iribarren number (ξ and ξ_o) also known as the surf similarity parameter. This parameter was introduced by Iribarren and Nogales (1949) as an indicator for whether breaking would occur on a plane slope. As discussed by Battjes (1974), the derivation of Iribarren and Nogales suggests the parameter ξ_o gives the ratio of the beach or structure slope "steepness" to the square root of wave steepness as defined by the local wave height (H) at the toe of the slope divided by the deepwater wave length (L_o). Note that often the parameter ξ_o is calculated using a finite-depth local wave height near the slope toe rather than a true deepwater H_o. For example, in laboratory experiments, it is common to specify H as the wave height measured over the flat-bottom portion of the wave facility before significant wave transformation occurs due to shoaling. In some cases, $H \approx H_o$, but this is not always assured. For the discussion in this paper, we will assume that ξ_o is based on the local wave height at or near the toe of the slope rather than H_o.

Hunt (1959) studied runup of regular waves on plane and composite slopes. His analysis for the case where waves break on the slope resulted in a dimensionally nonhomogeneous equation for maximum runup R given as

$$\frac{R}{H} = 2.3\frac{\tan\alpha}{\sqrt{\frac{H}{T^2}}} \tag{1}$$

Recognizing that the coefficient 2.3 has units of $ft^{1/2}/s$, Eq. (1) can be expressed as a dimensionally homogeneous equation in terms of deepwater Iribarren number with the introduction of the gravity constant in Imperial units, i.e.,

$$\frac{R}{H} = 1.0\xi_o \tag{2}$$

This form of Hunt's equation (with different dimensionless coefficient) is presently used to estimate irregular wave runup on plane impermeable slopes (De Waal and Van der Meer, 1992; Burcharth and Hughes, 2002).

The surf similarity parameter was popularized by Battjes (1974) who christened it as the Iribarren number and showed its applicability to a number of surf zone processes including: a criterion for wave breaking, differentiation of breaker types, wave setup, wave runup and rundown, wave reflection, and number of waves in the surf zone. Since that time, the Iribarren number has appeared in many empirical formulas related to beach processes and coastal structures.

The deepwater Iribarren number is directly proportional to the wave period and to the beach or structure slope, and ξ_o is inversely proportional to the square root of local wave height. Water depth is not included in the deepwater Iribarren number, but it is implicitly included in the local Iribarren number based on local wave length. Most successful applications of the deepwater Iribarren number pertain to surf zone processes where the waves undergo depth-limited breaking on the slope. Consider two waves having significantly different wave heights but the same value of wave steepness, H/L_o. Depth-limited breaking will occur at different depths on the slope, and the magnitude of the dimensional flow parameters at breaking will be different; but this does not seem to matter for some surf zone processes that are well correlated to ξ_o. As a simple approximation, waves in the surf zone decay in a self-similar manner with breaker height proportional to water depth, so it can be argued that the wave bores resulting from these two different waves behave much the same after breaking provided they have the same deepwater wave steepness prior to breaking. Likewise, we should expect somewhat similar flow characteristics in the broken waves as suggested by Battjes (1974).

However, prior to depth-limited wave breaking, deepwater wave steepness based on local wave height (and by extension the deepwater Iribarren number) is not necessarily a good descriptor of flow kinematics because local water depth is not included. This is illustrated by noting that deepwater wave steepness can be represented as the product of relative wave height (H/h) and relative water depth (h/gT^2), so that

$$\frac{\xi_o}{\tan\alpha} = \left(\frac{H}{L_o}\right)^{-1/2} = \left[2\pi\left(\frac{H}{h}\right)\left(\frac{h}{gT^2}\right)\right]^{-1/2} \tag{3}$$

Fig. 1 plots the variation of $(H/L_o)^{-1/2}$ for different values of relative depth. The solid lines are constant values of relative wave height (H/h) between 0.1 and 0.7. The heavy-dashed curve is the wave steepness

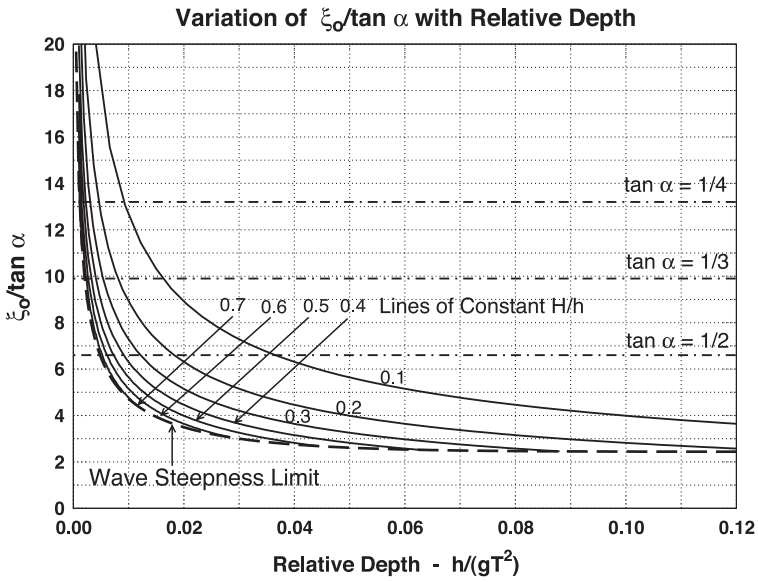

Fig. 1. Variation of $(H/L_o)^{-1/2}$ with h/gT^2 for constant values of H/h.

limit as defined by Williams (1985) and expressed by Sobey (1998) as a rational function. The horizontal chain-dashed lines represent the demarcation (ξ_o=3.3) between surging/collapsing breakers (above the line) and plunging/ spilling breakers (below the line) for different slopes. Similar trends arise if H/L_o is replaced with local wave steepness H/L.

Different combinations of H/h and h/gT^2 yield the same value of deepwater wave steepness. In particular, a wave in shallow water having the same height and period as a wave in deeper water will have the same deepwater wave steepness, but different wave kinematics. The wave in deeper water will behave more like a linear wave whereas the wave in shallow water will exhibit more nonlinearity. Furthermore, a change in wave height occurs as the deeper water wave moves into shallow water, so it is possible that by the time the deeper water waves reaches the depth of the shallow water wave, the wave height will be different. Thus, deepwater Iribarren number based on local wave height may not be the best parameter for correlations involving waves prior to breaking, or for waves described as surging or collapsing breakers, because the influence of water depth is not included. However, ample evidence supports the use of deepwater wave steepness H/L_o (and ξ_o) for correlations to surf zone processes due to plunging and spilling wave breaking.

3. Criteria for a new wave parameter

Partial motivation for developing a new wave parameter for nearshore coastal processes and coastal structure design comes from the Hudson armor stability equation and other stability equations based on the armor stability parameter, $H/\Delta D_{n50}$. Examination of Hudson's (1959) development of the stability equation reveals that wave height enters the armor stability parameter as a near-breaking long-wave approximation of horizontal water velocity in the vicinity of the still water level, i.e., $V_w \propto \sqrt{gH}$. From a physical perspective, this seems to be a gross simplification of wave effects on armor stability. However, because of other complexities related to armor stability (randomness of armor matrix, armor support points, interlocking, etc.), the lack of a more rigorous description for wave loading may not have been too detrimental. Most established stability coefficients for use with the Hudson equation were based on the more conservative observations rather than the mean of the data. Nevertheless, there remains the possibility that the observed scatter in armor

stability tests could be reduced with a more physically relevant parameter that better represents the wave forcing.

This paper describes development of a new wave parameter to represent the influence of nearshore waves in correlations between wave forcing and corresponding coastal processes. It is anticipated that this new wave descriptor will prove useful to depict processes that occur when waves impinge on coastal structures. The new wave parameter ideally will satisfy the following criteria:

(1) The parameter must be physically relevant so it can be incorporated into simple descriptive models of specific physical processes.
(2) The parameter should apply to both periodic waves and transient waves such as ship wakes and solitary waves with the hope that results from one wave type might be applicable for the other type.
(3) The parameter should span the range of relative depths from deep water to shallow water.
(4) The parameter should provide a better representation of nonbreaking and nonlinear wave processes than existing simple wave parameters.
(5) The parameter should provide comparable results to established parameters such as the Iribarren number when used to predict processes stemming from plunging and spilling wave breaking.
(6) The parameter should be easy to estimate so design guidance using the parameter can be programmed into computer spreadsheets or simple programs.

The following sections introduce a new parameter based on maximum wave momentum flux, and the parameter is developed for linear waves, nonlinear (Fourier approximation) waves, and solitary waves. The parameter is also estimated for a ship-generated wave, and use with irregular wave trains is discussed. No practical applications are given in this paper; but a companion paper (Hughes, 2004) demonstrates the utility of the proposed wave parameter by development of new empirical equations for runup of regular, irregular, and solitary waves on smooth, impermeable plane slopes. In addition, Melby and Hughes (2003) applied the new wave parameter to formulate equations for rock armor stability of rubble-mound coastal structures.

4. Maximum wave momentum flux—periodic waves

All wave theories are based on varying simplifications of the continuity and momentum equations, so it seems reasonable that a parameter representing the rate of change of wave momentum would be a good candidate for use in coastal structure design and for estimation of nearshore processes. Longuet-Higgins and Stewart (1964) noted the relevance of wave momentum flux. . .

"Surface waves possess momentum which is directed parallel to the direction of propagation and is proportional to the square of the wave amplitude. Now if a wave train is reflected from an obstacle, its momentum must be reversed. Conservation of momentum then requires that there be a force exerted on the obstacle, equal to the rate of change of wave momentum. This force is a manifestation of the radiation stress."

Thus, wave momentum flux is the property of progressive waves most closely related to force loads on coastal structures or any other solid object placed in the wave field. For this reason, wave momentum flux is a compelling wave property for characterizing waves in the nearshore region, and potentially, for relating waves to the response of coastal structures due to wave loading or to other coastal processes.

The relevance of wave momentum flux to wave runup on a beach was noted by Archetti and Brocchini (2002). They showed a strong correlation between the time series of wave runup and the time series of depth-integrated mass flux within the swash zone. They also noted that the local depth-integrated momentum flux was balanced mainly by the weight of water in the swash zone which was approximated as a triangular wedge. Their observation suggests that maximum wave runup on an impermeable slope might be directly proportional to the maximum depth-integrated wave momentum flux.

The instantaneous flux of horizontal momentum (m_f) across a unit area of a vertical plane oriented parallel to the wave crests is given by

$$m_f(x,z,t) = p_d + \rho u^2 \tag{4}$$

where p_d—instantaneous wave dynamic pressure at a specified position; u—instantaneous horizontal water velocity at the same specified position; ρ—water density.

Longuet-Higgins and Stewart (1964) defined the component of "radiation stress" perpendicular to the wave crest as the wave momentum flux integrated over the water depth and averaged over the wave, i.e.,

$$S_{xx} = \frac{1}{L}\int_0^L \int_{-h}^{\eta(x)} (p_d + \rho u^2)\mathrm{d}z\mathrm{d}x \tag{5}$$

They substituted linear (Airy) theory expressions for pressure and horizontal velocity and completed the integration by applying first-order wave kinematics above the still water level, which is not strictly first-order theory. This "extended linear theory" resulted in the expression

$$S_{xx} = \frac{1}{2}\rho g a^2\left(\frac{1}{2} + \frac{2kh}{\sinh 2kh}\right) \tag{6}$$

where L—local wave length; h—water depth from bottom to the still water level; η—instantaneous sea surface elevation relative to still water level; z—vertical coordinate directed positive upward with origin at the SWL; x—horizontal coordinate positive in the direction of wave propagation; g—gravitational acceleration; a—wave amplitude; k—wave number [$=2\pi/L$]. Note that S_{xx} has units of force per unit length of wave crest.

There is significant variation of depth-integrated wave momentum flux over a wave length from large positive values at the crest to large negative values in the trough. So instead of adopting a wave-averaged value (i.e., S_{xx}) which is quite small compared to the range of variation, it is logical when considering some coastal processes, such as the wave force loading on structures, to focus on the maximum, depth-integrated wave momentum flux that occurs during passage of a wave, i.e., the maximum of

$$M_F(x,t) = \int_{-h}^{\eta(x)} (p_d + \rho u^2)\mathrm{d}z \tag{7}$$

that occurs at the wave crest when $\eta(x)=a$. Note that on the surface of a perfectly reflecting, impermeable vertical wall, the horizontal velocity u is zero, and Eq. (7) becomes simply the integral over the water depth of the dynamic pressure exerted by the wave on the wall, or the total instantaneous wave force on the wall (excluding the hydrostatic pressure component).

Maximum depth-integrated wave momentum flux, as defined by Eq. (7) with $\eta(z)=a$, can be determined for any surface wave form provided the velocity and pressure field under the crest can be specified. In theory, this means that a wave parameter based on momentum flux has the potential of applying to both periodic and transient wave types, which may be a useful property. More importantly, the physical relevance of wave momentum flux to force loading on structures seems logical, thus fulfilling an important criterion for the proposed wave parameter.

4.1. Linear (Airy) wave theory

In linear wave theory, dynamic pressure and horizontal wave velocity are in phase with the sea surface elevation, and the maximum wave momentum flux occurs at the wave crest. The first-order approximation of depth-integrated wave momentum flux is found by substituting the dynamic pressure and horizontal wave velocity at the wave crest from Airy wave theory into Eq. (7) and integrating from the bottom only up to the still water level because kinematics are not specified above still water level in first-order theory. From linear wave theory with no unidirectional current,

$$p_d(z)_{\mathrm{crest}} = \rho g a \frac{\cosh k(h+z)}{\cosh kh} \tag{8}$$

and

$$u(z)_{\mathrm{crest}} = \alpha\omega \frac{\cosh k(h+z)}{\sinh kh} \tag{9}$$

where ω is circular wave frequency ($=2\pi/T$), and T is wave period. Strictly, the dynamic pressure term should also include a vertical velocity component ($-\rho w^2$), so the dynamic pressure is at the same level of approximation as the horizontal velocity term. However, at the wave crest, $w=0$ throughout the water column and contributes nothing to the dynamic pressure; therefore, the term is not included here.

Substituting Eqs. (8) and (9) into Eq. (7) and integrating from the bottom to the still water level yields the analytically continuous expression

$$(M_F)_{max} = \frac{\rho g a}{k}\frac{\sinh kh}{\cosh kh} + \frac{\rho a^2\omega^2}{4k}\frac{\sinh 2kh + 2kh}{\sinh^2 kh} \tag{10}$$

The second term in Eq. (10) is simplified by substituting the linear dispersion relationship $\omega^2 = gk \tanh kh$ and making use of the identity $\sinh kh \times \cosh kh = 1/2 \sinh 2kh$. Thus, the first-order theory approximation for maximum depth-integrated wave momentum flux is given by

$$(M_F)_{max} = \frac{\rho g a}{k}\tanh kh + \frac{\rho g a^2}{2}\left[1 + \frac{2kh}{\sinh 2kh}\right] \tag{11}$$

which, like S_{xx}, has units of force per unit length of wave crest.

A convenient expression for nondimensional maximum depth-integrated wave momentum flux arises by dividing Eq. (11) by ($\rho g h^2$) and recognizing wave height H is twice the wave amplitude, a, i.e.,

$$\left(\frac{M_F}{\rho g h^2}\right)_{max} = \frac{1}{2}\left(\frac{H}{h}\right)\frac{\tanh kh}{kh} + \frac{1}{8}\left(\frac{H}{h}\right)^2 \times \left[1 + \frac{2kh}{\sinh 2kh}\right] \tag{12}$$

For convenience, the nondimensional depth-integrated maximum wave momentum flux, given as

$$\left(\frac{M_F}{\rho g h^2}\right)_{max}$$

will be referred to as simply the "wave momentum flux parameter."

Eq. (12) expresses the wave momentum flux parameter as a function of relative wave height (H/h) and relative depth (kh). Fig. 2 presents the nondimensional parameter for a family of curves representing constant values of H/h. The abscissa on the plot is the commonly used relative depth, h/gT^2. For a constant water depth, wave period increases toward the left and decreases to the right. The range of relative depths covers most coastal applications. The dashed line gives the steepness-limited wave-breaking criterion

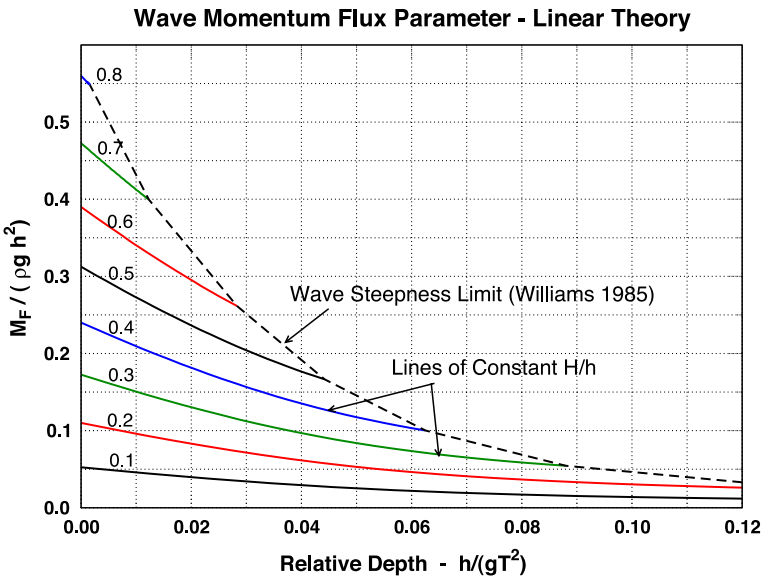

Fig. 2. Wave momentum flux parameter versus h/gT^2 (linear wave theory).

tabulated by Williams (1985) and expressed by Sobey (1998) as the rational approximation

$$\frac{\omega^2 H_{\text{limit}}}{g} = c_o \tanh\left(\frac{a_1 r + a_2 r^2 + a_3 r^3}{1 + b_1 r + b_2 r^2}\right) \tag{13}$$

where $r=\omega^2 h/g$, a_1=0.7879, a_2=2.0064, a_3=−0.0962, b_1=3.2924, b_2=−0.2645, and c_o=1.0575. Sobey noted the above expression has a maximum error of 0.0014 over range of Williams' table. Williams' (1985) tabulation of limit waves is more accurate than the traditional limit steepness given by

$$\frac{H_{\text{limit}}}{L} = 0.142 \tanh(kh) \tag{14}$$

Eq. (14) overestimates limiting steepness for long waves and underestimates limiting steepness for short waves.

The relative contribution of the velocity term (ρu^2) to the total depth-integrated wave momentum flux varies between about 5% for low-amplitude long-period waves to nearly 30% for waves approaching limiting steepness. Linear theory estimates of maximum depth-integrated wave momentum flux are lower than actual because the momentum flux above the still water level is neglected.

As the wave period increases, and the wave length becomes very long (shallow water waves), the wave number approaches zero, and Eq. (12) approaches a limiting value for the wave momentum flux parameter given by

$$\left(\frac{M_F}{\rho g h^2}\right)_{\max} = \frac{1}{2}\left(\frac{H}{h}\right) + \frac{1}{4}\left(\frac{H}{h}\right)^2 \quad \text{(for very short waves)} \tag{15}$$

This limit is evident on the ordinate axis of Fig. 2. Similarly, Eq. (12) approaches an asymptotic form for very short period waves given by

$$\left(\frac{M_F}{\rho g h^2}\right)_{\max} = \frac{1}{8\pi^2}\left(\frac{H}{h}\right)\left(\frac{h}{gT^2}\right)^{-1} + \frac{1}{8}\left(\frac{H}{h}\right)^2 \quad \text{(for very short waves)} \tag{16}$$

However, this deepwater limit is of little interest when considering nearshore coastal processes or coastal structures.

4.2. Extended linear wave theory

By assuming expressions for linear theory wave kinematics are valid above the still water level, it is possible to derive a somewhat more accurate estimate of maximum depth-integrated wave momentum flux at the wave crest. This technique has been referred to as extended linear theory or one-and-a-half-order wave theory.

Substituting Eqs. (8) and (9) for p_d and u, respectively, in Eq. (7), integrating from $z=-h$ to $z=a$ (wave crest), applying the dispersion relation $\omega^2=gk \tanh kh$, and making use of the identity $\sinh kh \cosh kh=1/2 \sinh 2kh$ as before yields

$$(M_F)_{\max} = \frac{\rho g a}{k}\frac{\sinh[k(h+a)]}{\cosh(kh)} + \frac{\rho g a^2}{2} \times \left[\frac{\sinh[2k(h+a)] + 2k(h+a)}{\sinh 2kh}\right] \tag{17}$$

Dividing Eq. (17) by ($\rho g h^2$) and substituting $a=H/2$ gives the nondimensional form of the maximum depth-integrated wave momentum flux parameter for extended linear theory, i.e.,

$$\left(\frac{M_F}{\rho g h^2}\right)_{\max} = \frac{1}{2}\left(\frac{H}{h}\right)\frac{\sinh[k(h+H/2)]}{kh\cosh(kh)} + \frac{1}{8}\left(\frac{H}{h}\right)^2 \times \left[\frac{\sinh[2k(h+H/2)] + 2k(h+H/2)}{\sinh 2kh}\right] \tag{18}$$

The asymptotic long-wave limit of Eq. (18) as $k \to 0$ is given by

$$\left(\frac{M_F}{\rho g h^2}\right)_{\max} = \left[\frac{1}{2}\left(\frac{H}{h}\right) + \frac{1}{4}\left(\frac{H}{h}\right)^2\right] \times \left[1 + \frac{1}{2}\left(\frac{H}{h}\right)\right] \quad \text{(for very long waves)} \tag{19}$$

which is seen to be an extension of the linear theory long-wave limit.

Fig. 3 plots the extended linear theory solution for the wave momentum flux parameter as a function of relative depth h/gT^2. The limiting wave steepness, as

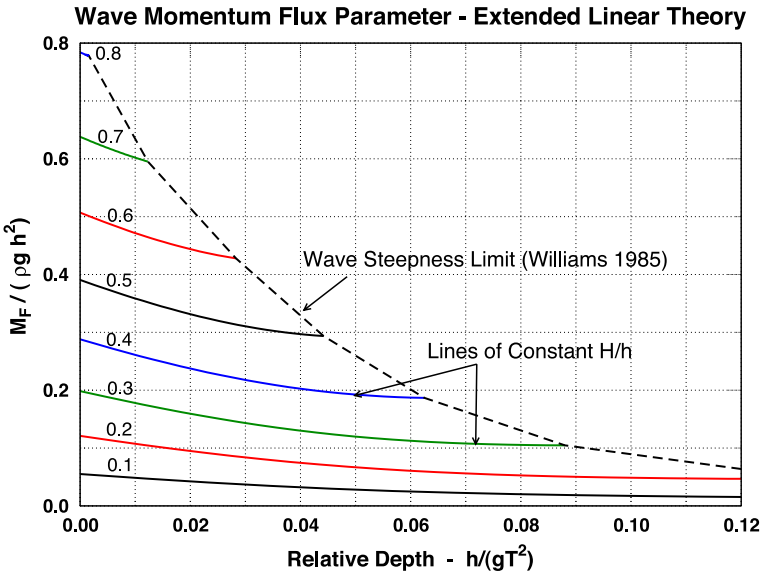

Fig. 3. Wave momentum flux parameter versus h/gT^2 (extended linear wave theory).

given by Williams (1985), is shown by the dashed line. Percentage contributions from the pressure and horizontal velocity terms were similar to those noted for linear theory. As expected, estimates of maximum depth-integrated wave momentum flux are greater than corresponding estimates from linear theory with the largest increase of almost 30% occurring for long waves near the steepness limit. Extended linear theory gives better estimates of $(MF)_{\max}$ than linear theory, but it still does not account for wave asymmetry about the horizontal axis characterized by peaked crests and long, shallow troughs typical of nonlinear waves.

4.3. Nonlinear (Fourier) wave theory

Although linear and extended linear wave theories provide simple analytical estimates of maximum depth-integrated wave momentum flux, experience tells us that the momentum flux contained in the wave crest is crucial if we wish to relate this parameter to the response of coastal structures in a realistic way. The linear theory estimate of maximum wave momentum flux omits that portion of momentum flux above the still water line, and the extended linear theory neglects the effects of nonsinusoidal wave forms typical of nonlinear, shallow water waves. These omissions will become more problematic as the wave approaches its limiting relative wave height (H/h).

Fourier approximation wave theory (Rienecker and Fenton, 1981; Fenton, 1988; Sobey, 1989) provides good characterization of steady, finite-amplitude waves of permanent form over the entire range of water depths from deepwater to nearshore and for wave heights approaching the limiting steepness. This hybrid analytical/computational methodology represents the wave stream function by a truncated Fourier series that exactly satisfies the field equation (Laplace), the kinematic bottom boundary condition, and the lateral periodicity boundary conditions. Nonlinear optimization is used to complete the solution by determining values for the remaining unknowns that best satisfy the nonlinear kinematic and dynamic free surface boundary conditions (Sobey, 1989). Generally, more terms are needed in the truncated Fourier series to represent waves with pronounced asymmetry about the still water line, i.e., steep waves and shallow water waves. Once the coefficients of the Fourier series are established for a particular wave, the kinematics for the entire wave can be easily calculated.

Because Fourier approximation wave theory provides complete kinematics for finite amplitude waves spanning the range covered by Stokes and Cnoidal

wave theories, it is possible to estimate reasonable values for maximum depth-integrated wave momentum flux associated with these waves. Unfortunately, such estimates of $(MF)_{max}$ must be calculated numerically which could significantly lessen the utility of the wave momentum flux parameter for design purposes.

A simple empirical approximation for the wave momentum flux parameter of finite amplitude waves was developed using a Fourier wave computer program. This program was repeatedly run for selected combinations of wave steepness (H/h) and relative depth (h/gT^2), and the resulting estimates of wave kinematics were used to calculate maximum depth-integrated wave momentum flux according to Eq. (7). Results are presented as the set of curves shown on Fig. 4. Coding accuracy was checked by assuring that estimates of $(MF)_{max}$ for small amplitude, deepwater waves were the same as estimates given by the first-order analytical solution. In addition, it was noted that estimates for very long waves (small values of h/gT^2) approached the values obtained from the analytical solitary wave solution given in the following section. The dashed line on the plot represents the limiting wave steepness given by Williams (1985).

The difference between linear, extended linear, and finite-amplitude theory estimates of the wave momentum flux parameter is illustrated on Fig. 5 which shows curves representing H/h=0.3 and 0.7. For the lower relative wave height of H/h=0.3, there is good correspondence between extended linear and Fourier approximation for values of h/gT^2 greater than about 0.03. As the relative depth decreases from 0.03, there is increasing divergence which illustrates the importance of nonlinear wave shape. Linear theory under predicts extended linear theory by nearly a constant amount.

For relatively high waves (H/h=0.7), linear and extended linear estimates clearly underpredict the correct value of the wave momentum flux parameter. For example, at a value of h/gT^2=0.01, the Fourier approximation estimate of dimensionless $(MF)_{max}$ is 2.0 times greater then the linear estimate and 1.4 times greater than the extended linear estimate. This difference increases as relative depth decreases, emphasizing the importance of nonlinearities in nearshore waves.

Application of the wave momentum flux parameter to coastal structure design and estimation of coastal processes will typically involve empirical correlation of the parameter with observed responses. It could be argued that the empirical nature of this type of application does not depend on absolute values but rather on relative values of the incorporated wave parameter; and in general, the linear and extended linear curves show similar trends as the finite-

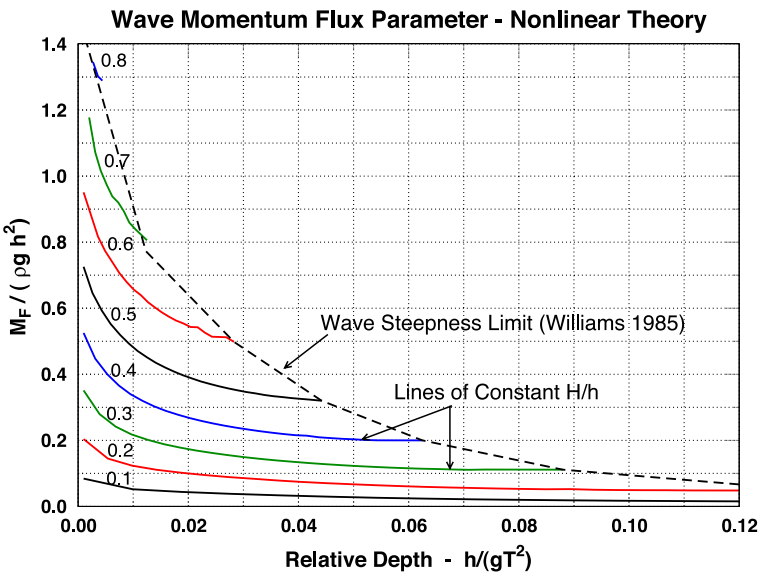

Fig. 4. Wave momentum flux parameter versus h/gT^2 (Fourier wave theory).

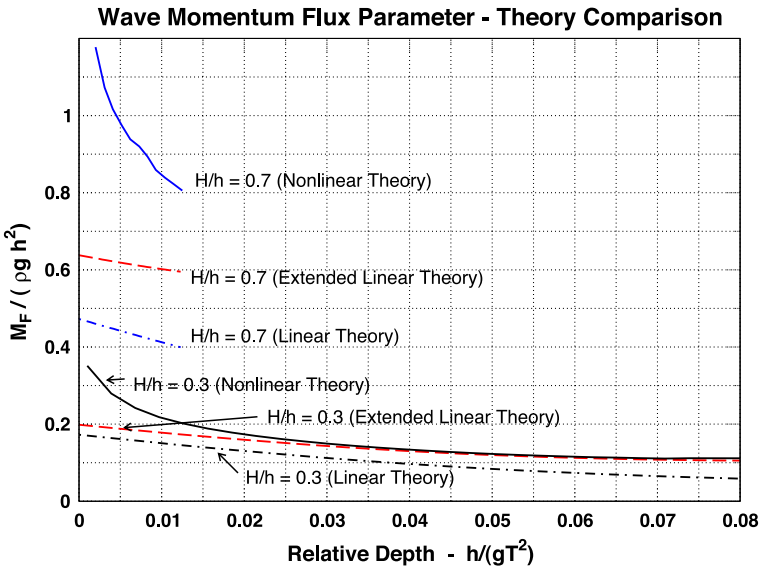

Fig. 5. Comparison of linear, extended linear, and finite-amplitude wave momentum flux parameters.

amplitude curves. Thus, the simpler, analytical linear theories could be used without significant loss of validity, provided the same linear theory was used for all cases. However, one of the stated criteria for this new parameter is that it must be useful for regular waves, irregular waves, and nonperiodic waves. By using the best estimate of $(MF)_{\max}$ for each category of wave, it may be possible in the future to relate design guidance established for one type of wave to similar circumstances involving other wave types. For example, if rubble-mound armor stability can be related to $(MF)_{\max}$ for regular waves, then it may be possible to extend the stability prediction to structures exposed to transient ship-generated waves or solitary waves simply by estimating the maximum depth-integrated wave momentum flux for the other type of wave. For this reason, it is suggested that estimates of $(MF)_{\max}$ for regular periodic waves be made using the Fourier approximation method.

An empirical equation for estimating the wave momentum flux parameter for finite amplitude steady waves was established using the calculated curves of constant H/h shown in Fig. 4. A nonlinear best-fit of a two-parameter power curve was performed for each calculated H/h curve. Next, the resulting power curve coefficients and exponents were plotted as a function of H/h, and fortunately, both the coefficients and exponents could be reasonably represented by power curves. The resulting, purely empirical equation representing the curves shown on Fig. 4 is given as

$$\left(\frac{M_{\mathrm{F}}}{\rho g h^2}\right)_{\max} = A_0\left(\frac{h}{gT^2}\right)^{-A_1} \tag{20}$$

where

$$A_0 = 0.6392\left(\frac{H}{h}\right)^{2.0256} \tag{21}$$

$$A_1 = 0.1804\left(\frac{H}{h}\right)^{-0.391} \tag{22}$$

Although the empirical coefficients and exponents in Eqs. (21) and (22) are expressed to four decimal places, corresponding accuracy is not implied. Rounding to two decimal places should be reasonably adequate for practical application of these empirical equations.

Goodness-of-fit of Eq. (20) compared to the computed values given on Fig. 4 is shown on Fig. 6. For smaller values of nondimensional $(MF)_{\max}$, there is reasonable correspondence except for the left-most points of each curve (shown below the line of equivalence). This divergence was caused by the power curve tending toward positive infinity as $h/gT^2 \rightarrow 0$. However, greater deviation begins to occur for dimensionless $(MF)_{\max} > 0.6$. Nevertheless, the only poorly fitted curve is for $H/h = 0.8$ which is at

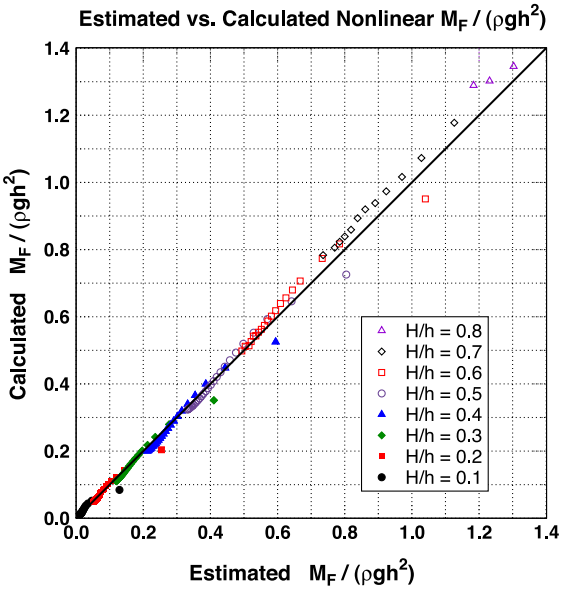

Fig. 6. Goodness-of-fit of nonlinear momentum flux empirical equation (Fourier wave theory).

or slightly above the limiting relative wave height for waves on a horizontal seabed. This problem was likely the result of forcing the numerical computation beyond appropriate limits. The maximum underprediction and overprediction of the empirical curve-fit were 0.105 and 0.089, respectively. The overall root-mean-squared error of the curve-fit was 0.023.

The empirical equation represented by Eq. (20), along with Eqs. (21) and (22), provides an easy method for estimating the wave momentum flux parameter for finite-amplitude, steady regular waves. This empirical formulation is recommended over those provided by linear and extended linear theory because it better represents the momentum flux in the wave crest which is expected to be critical for most applications to coastal structures.

4.4. Application to irregular waves

Most coastal structure design guidance developed in the past 20–25 years use wave parameters representative of unidirectional irregular wave trains or, in rarer cases, directionally spread irregular waves. Attempts have been made to relate the irregular wave parameters to regular wave counterparts, but no uniform, clear consensus has been found.

The wave momentum flux parameter representing an irregular wave train is probably best specified by direct substitution of irregular wave parameters into the empirical Eqs. (20), (21), and (22) developed using Fourier approximation theory. Application is simple, and estimates of maximum wave momentum flux should be reasonably representative of the irregular wave train. One drawback to this method is inconsistency between investigators regarding which irregular wave parameters to substitute. One application may use time–domain statistics $H_{1/3}$ and T_m, while another might use frequency–domain parameters H_{mo} and T_p. Thus, it is important to specify clearly which irregular wave representative wave height and period are substituted. For now, the direct correspondence by substitution of irregular wave parameters H_{mo} and T_p is recommended for estimating a value of the wave momentum flux parameter representative of irregular waves.

5. Maximum wave momentum flux—transient waves

Because the maximum, depth-integrated wave momentum flux can be determined for any wave form in which the kinematics are known, it is possible to estimate the wave momentum flux parameter for nonperiodic waves. This may prove useful for comparing coastal process responses for different wave types.

5.1. Solitary wave theory

The maximum depth-integrated wave momentum flux of a solitary wave occurs at the crest where both the horizontal velocity and dynamic pressure are greatest. To first-order of approximation, the horizontal velocity at the crest as a function of elevation z_s above the bottom can be approximated as (e.g., Wiegel, 1964)

$$u_{\max}(z_s) = \frac{CN}{[1 + \cos(\frac{Mz_s}{h})]} \tag{23}$$

and the total pressure, which is given at first order as hydrostatic, is expressed as a function of z_s at the crest as

$$P_T(z_s) = \rho g(\eta_s - z_s) = \rho g[(H+h) - z_s] \tag{24}$$

where C—solitary wave celerity $[=\sqrt{g(H+h)}]$; η_s—sea surface elevation measured from the sea floor; z_s—vertical coordinate-directed positive upward with origin at the sea floor; h—water depth from the bottom to still water level; M, N—coefficients that are functions of H/h.

Because the reference coordinate system has its origin on the sea floor, the depth-integrated momentum flux definition equation changes slightly to

$$M_F(x) = \int_0^{\eta(x)} (p_d + \rho u^2)\mathrm{d}z_s \tag{25}$$

and the maximum depth-integrated wave momentum flux for a solitary wave is found as

$$(M_F)_{max} = \int_0^{(H+h)} \rho g[(H+h) - z_s]\mathrm{d}z_s - \int_0^h \rho g z_s \mathrm{d}z_s + \int_0^{(H+h)} \rho \frac{C^2N^2}{\left[1+\cos\left(\frac{Mz_s}{h}\right)\right]^2}\mathrm{d}z_s \tag{26}$$

The first integral in Eq. (26) is the total pressure, and the second integral is the hydrostatic pressure between the bottom and the still water level. Subtracting the second integral from the first results in depth-integrated wave dynamic pressure. Performing the integration and substituting for wave celerity, C, results in the expression

$$(M_F)_{max} = \frac{\rho g}{2}(H^2 + 2Hh) + \frac{\rho g}{2}\frac{(H+h)N^2h}{M}\left\{\tan\left[\frac{M}{2}\left(\frac{H}{h}+1\right)\right] + \frac{1}{3}\tan^3\left[\frac{M}{2}\left(\frac{H}{h}+1\right)\right]\right\} \tag{27}$$

Dividing both sides by $\rho g h^2$ yields the nondimensional expression for the wave momentum flux parameter

$$\left(\frac{M_F}{\rho g h^2}\right)_{max} = \frac{1}{2}\left[\left(\frac{H}{h}\right)^2 + 2\left(\frac{H}{h}\right)\right] + \frac{N^2}{2M}\left(\frac{H}{h}+1\right)\left\{\tan\left[\frac{M}{2}\left(\frac{H}{h}+1\right)\right] + \frac{1}{3}\tan^3\left[\frac{M}{2}\left(\frac{H}{h}+1\right)\right]\right\} \tag{28}$$

The first bracketed term in Eq. (28) arises from the dynamic pressure, and interestingly, this term is exactly twice the value of the long wave approximation of the wave momentum flux parameter derived from linear wave theory and shown in Eq. (15). The second term represents the contribution of horizontal velocity to the wave momentum flux parameter.

The coefficients M and N are typically presented in graphical form (e.g., Wiegel, 1964; Shore Protection Manual, 1984). To accommodate calculations, a nonlinear curve fit was applied to the plotted curves to produce the following simple equations that give reasonable values for M and N

$$M = 0.98\left\{\tanh\left[2.24\left(\frac{H}{h}\right)\right]\right\}^{0.44} \tag{29}$$

$$N = 0.69\tanh\left[2.38\left(\frac{H}{h}\right)\right] \tag{30}$$

The empirically fit equations (solid lines) are plotted along with the data points taken from the Shore Protection Manual (1984) on Fig. 7. Maximum underprediction and overprediction errors for Eq. (29) are 0.018 and 0.023, respectively. Overall, root-mean-squared error is 0.010. Eq. (30) has maximum under- and over-prediction errors of 0.010 and 0.006, respectively, with overall root-mean-squared error of 0.0056.

The variation of the wave momentum flux parameter for solitary waves as a function of H/h is shown in Fig. 8. These values represent the upper limit of the nonlinear (Fourier) wave case when $h/(gT^2)$ approaches zero (see Fig. 4). At a value of H/h=0.1, the velocity term contributes only about 7% of the calculated momentum flux, whereas as at H/h=0.8, the percentage increases to around 38% of the total. It

should be possible to perform a similar derivation for higher order solitary wave theory, but estimates of maximum depth-integrated wave momentum flux from higher-order theory are not expected to be markedly different from results obtained from first-order solitary theory.

5.2. Nonlinear ship-generated waves

Applying common periodic wave parameters to transient waves such as ship-generated waves requires that individual waves in the wave train be identified and treated as uniform waves of permanent form. For example, Fig. 9 shows a transient ship-generated wave from a laboratory experiment. One of the highest waves has been defined as the crest and trough between two successive zero upcrossings of the still water level. The period for this wave is the time between the two upcrossings, and the wave height is the vertical distance between crest and following trough. However, does this nonlinear ship wave have the same effect on a coastal structure or on a shoreline as the nonlinear regular wave defined by the values of H and T? Intuitively, we might expect similar effects if the transient and uniform waves had similar values of the wave momentum flux parameter.

A time series of depth-integrated wave momentum flux corresponding to the section of transient wave shown in the box in Fig. 9 was calculated using the local Fourier approximation method described by Sobey (1992). This method is similar to the Fourier steady wave approximation method discussed earlier in this paper. The measured trace of sea surface elevations is subdivided into small sections, and for each subsection a stream function represented by a truncated Fourier series is defined. An optimal solution is found within each window that best satisfies the nonlinear free-surface kinematic and dynamic boundary conditions. Once kinematics are known throughout the water column, the wave momentum flux can be estimated at each point.

Smith and Swan (2002) compared exact numerical solutions of specified test cases to existing, less computationally intensive techniques for estimating kinematics of extreme waves. A favorable comparison was noted for Sobey's (1992) local Fourier approximation in the crest region near the sea surface, with less-favorable correspondence farther down in the water column. Because the maximum wave momentum flux is concentrated in the wave crest, the local Fourier approximation method is appropriate for estimating depth-integrated wave momentum flux for transient wave trains.

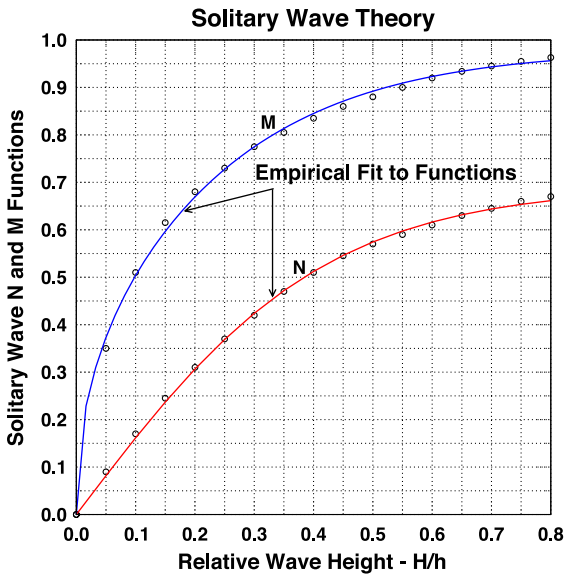

Fig. 7. Nonlinear curve fit to solitary wave N and M functions.

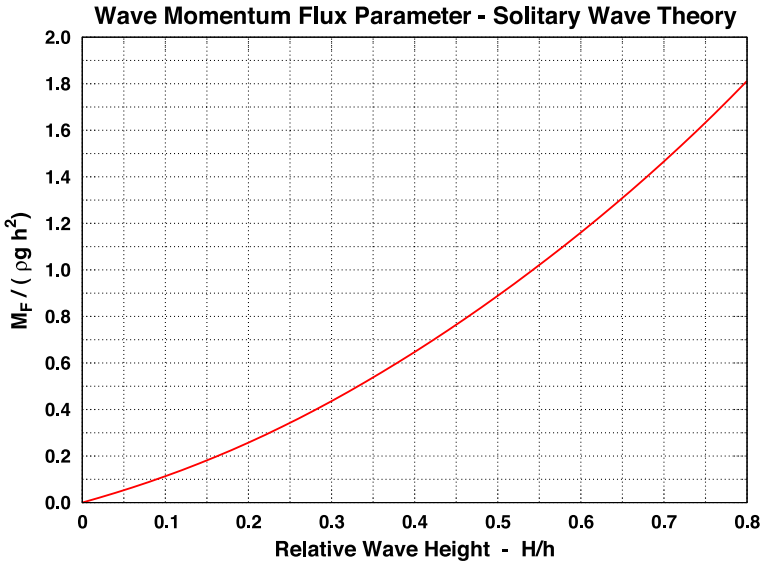

Fig. 8. Solitary wave momentum flux parameter versus H/h.

The upper plot of Fig. 10 shows the sea surface trace from the section of transient wave shown in the box in Fig. 9, and the lower plot is depth-integrated wave momentum flux calculated using the local Fourier approximation of Sobey. The time-dependent M_F is reasonably smooth near the crest, but the method is known to have difficulties in the trough and around the still water level where the sea surface curvature is small (see Sobey, 1992). No filtering was used during the computation. Despite problems resolving M_F away from the wave crest, the values for maximum depth-integrated wave momentum flux at the crest are considered to be valid.

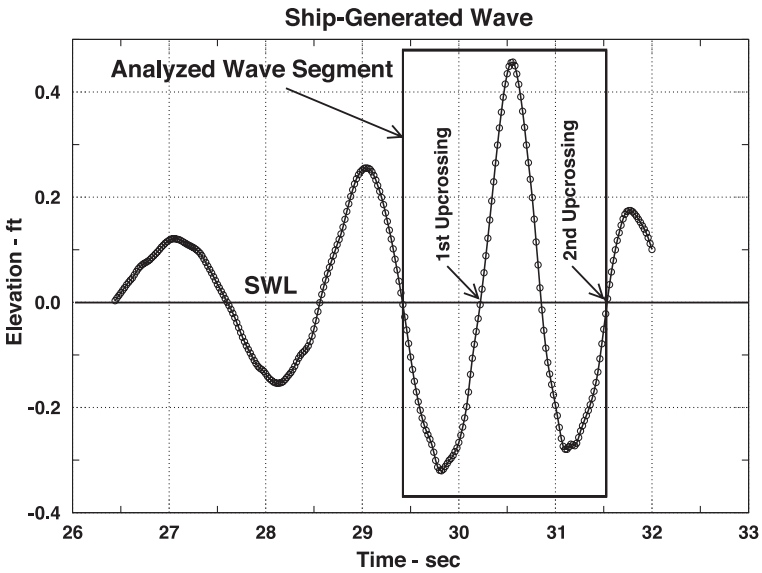

Fig. 9. Ship-generated transient wave time series from laboratory experiment.

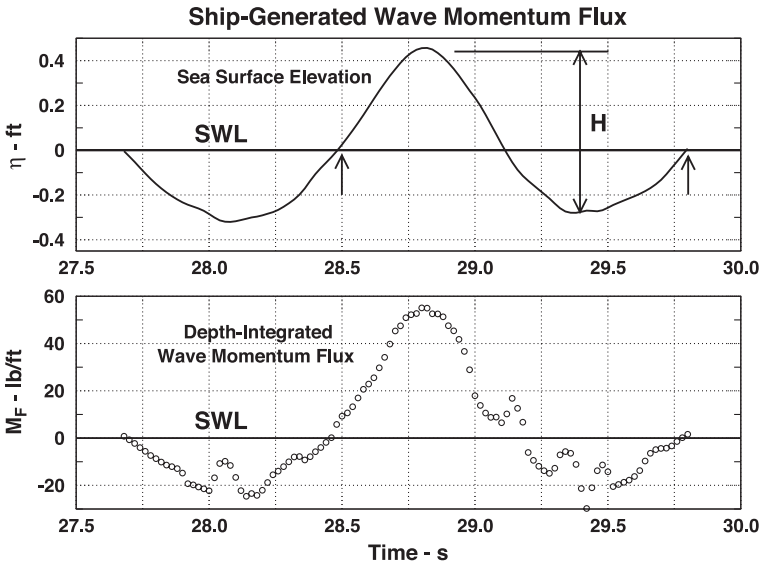

Fig. 10. Ship-generated wave sea surface (upper) and M_F (lower) time series.

An alternative estimate of maximum depth-integrated wave momentum flux for the individual wave defined by zero-upcrossings in Fig. 10 was calculated using Eqs. (20), (21), and (22) which are intended for regular steady waves. The wave parameters were originally given in English units as H=0.78 ft, T=1.38 s, and h=9 ft. A somewhat favorable comparison to the local Fourier approximation was found...

$$(M_F)_{max} = \begin{cases} 55.1\ lb/ft & \text{local approx.} \\ 48.7\ lb/ft & Eq.\ (20) \end{cases}$$

or

$$\left(\frac{M_F}{\rho g h^2}\right)_{max} = \begin{cases} 0.0106 & \text{local approx.} \\ 0.0094 & Eq.\ (20) \end{cases} \tag{31}$$

Although this is only one comparison, it may indicate that treating transient wave trains as a succession of uniform waves might be reasonable for those processes thought to be related to wave momentum flux.

6. Summary and conclusions

A new parameter representing the maximum depth-integrated wave momentum flux occurring in a wave is proposed for characterizing the wave contribution to nearshore coastal processes on beaches and at coastal structures. The wave momentum flux parameter has units of force per unit crest width, and it better characterizes the flow kinematics at a given depth than other wave parameters that do not distinguish increased wave nonlinearity. The wave momentum flux parameter can be defined for regular, irregular, and nonperiodic (transient) waves such as ship-generated wakes and solitary waves. Thus, if a nearshore process can be successfully related to the wave momentum flux parameter, it may be possible to describe the same process being forced by different wave types with a similar formulation. This hypothesis is presently unproven.

The wave momentum flux parameter was derived for linear and extended linear wave theory; however, the results do not accurately estimate the maximum wave momentum flux in steep, nonsinusoidal waves which are likely to be more influential for coastal process response. Fourier approximation wave theory for regular steady waves over a horizontal bottom was used to develop an easily applied empirical expression giving nondimensional maximum depth-integrated wave momentum flux as a function of relative wave height and relative water depth. For irregular wave trains, it is recommended that H and T in the empirical formation be replaced with frequency–domain irregular wave parameters H_{mo} and T_p. The wave

momentum flux parameter was also derived for first-order solitary wave theory, and a time-series of depth-integrated wave momentum flux was estimated for a transient ship-generated wave.

It is anticipated that the wave momentum flux parameter may prove useful for developing improved semiempirical formulas to describe nearshore processes and wave/structure interactions such as wave runup, overtopping, reflection, transmission, and armor stability. Surf zone processes where waves break as plunging or spilling breakers may not benefit from use of the wave momentum flux parameter because the breaking processes effectively negates the advantage of characterizing the wave nonlinearity. In these situations, use of the new parameter may not improve upon existing correlations to wave parameters such as the Iribarren number. However, for nonbreaking conditions or where wave breaking occurs as surging or collapsing breakers on steep slopes, the wave momentum flux parameter should, in theory, provide a better characterization of the wave forcing and lead to better process response correlations. This remains to be seen.

The optimism expressed in this paper regarding the utility of the new parameter is justified initially by reasonable correspondence of between the wave momentum flux parameter and wave runup on smooth, impermeable slopes (Hughes, 2004) and by new expressions for rubble-mound armor layer stability as functions of the wave momentum flux parameter (Melby and Hughes, 2003).

Notation

a wave amplitude
a_1, a_2, a_3 empirical coefficients
A_0 empirical coefficient
A_1 empirical exponent
b_1, b_2 empirical coefficients
c_o empirical coefficient
C solitary wave celerity $\left[=\sqrt{g(H+h)}\right]$
D_{n50} equivalent cube length of the median armor stone
g gravitational acceleration
h water depth from bottom to the still water level
H uniform steady wave height
H_{limit} steepness limit wave height
H_{mo} zeroth-moment wave height related to the area beneath the spectrum
H_{o} deepwater uniform wave height
H_{rms} root-mean-squared wave height for irregular wave train
H_{s} significant wave height for irregular wave train
$H_{1/3}$ average of the highest 1/3 waves in an irregular wave train
$H_{10\%}$ irregular wave height at which 10% of the waves are higher
k wave number $[=2\pi/L]$
L local wave length
L_{m} wave length associated with mean irregular wave period T_{m}
L_{o} deepwater wave length
L_{om} deepwater wave length associated with mean irregular wave period T_{m}
L_{op} deepwater wave length associated with peak spectral period T_{p}
L_{p} wave length associated with peak spectral period T_{p}
m_{f} instantaneous flux of horizontal momentum across a unit area
M coefficient for solitary wave theory (function of H/h)
M_F depth-integrated wave momentum flux across a unit width
$(M_F)_{\mathrm{max}}$ maximum depth-integrated wave momentum flux across a unit width
N coefficient for solitary wave theory (function of H/h)
p_{d} instantaneous wave dynamic pressure at a specified position
P_{T} total instantaneous wave pressure
r dimensionless water depth $[=\omega^2 h/g]$
R maximum vertical runup from SWL
S_{xx} wave-averaged momentum flux (also known as radiation stress)
t time
T wave period
T_{p} wave period associated with the spectrum peak frequency
T_{m} mean wave period in irregular wave train
u instantaneous horizontal water velocity at a specified position
V_{w} representative horizontal velocity near the still water level
x horizontal coordinate positive in the direction of wave propagation
z vertical coordinate directed positive upward with origin at the SWL

z_s vertical coordinate directed positive upward with origin at the sea floor

Greek Symbols

α beach or structure slope
Δ armor unit immersed relative density
η instantaneous sea surface elevation relative to still water level
η_s instantaneous sea surface elevation relative to the sea floor
μ coefficient of dynamic viscosity
ν coefficient of kinematic viscosity
ξ local Iribarren number (surf similarity parameter)
ξ_o deepwater Iribarren number
π mathematical Pi
ρ mass density of water
ω circular wave frequency [$=2\pi/T$]

Acknowledgements

The research described and the results presented herein, unless otherwise noted, were obtained from research funded through the Scour Holes at Inlet Structures work unit of the Coastal Inlets Research Program at the US Army Engineer Research and Development Center, Coastal and Hydraulics Laboratory (CHL). Permission was granted by Headquarters, U.S. Army Corps of Engineers, to publish this information.

Special thanks to Prof. Rodney J. Sobey, Imperial College London, for providing his Fourier approximation theory and local Fourier approximation theory source codes. The author is especially indebted to the journal reviewers for their useful suggestions and encouragement.

References

Archetti, R., Brocchini, M., 2002. An integral swash zone model with friction: an experimental and numerical investigation. Coastal Engineering vol. 45. Elsevier, pp. 89–110.

Battjes, J.A., 1974. Surf Similarity. Proceedings of the 14th International Coastal Engineering Conference vol. 1. American Society of Civil Engineers, pp. 466–480.

Burcharth, H.F., Hughes, S.A., 2002. Fundamentals of design. In: Hughes, S.A. (Ed.), Coastal Engineering Manual, Part VI, Design of Coastal Project Elements, Chapter VI-5, Engineer Manual 1110-2-1100. U.S. Army Corps of Engineers, Washington, DC.

De Waal, J.P., Van der Meer, J.W., 1992. Wave Runup and Overtopping on Coastal Structures. Proceedings of the 23rd International Coastal Engineering Conference vol. 2. American Society of Civil Engineers, pp. 1758–1771.

Fenton, J.D., 1988. The numerical solution of steady water wave problems. Computers & Geosciences vol. 14. Pergamon Press, Great Britain, pp. 357–368.

Hudson, R.Y., 1959. Laboratory investigation of rubble-mound breakwaters. Journal of the Waterways and Harbors Division vol. 85 (WW3). American Society of Civil Engineers, pp. 93–121.

Hughes, S.A., 2004. Estimation of wave runup on smooth, impermeable slopes using the wave momentum flux parameter. Coastal Engineering. in press [doi:10.1016/j.coastaleng.2004.07.026].

Hunt, I.A., 1959. Design of seawalls and breakwaters. Journal of the Waterways and Harbors Division vol. 85 (WW3). American Society of Civil Engineers, pp. 123–152.

Iribarren, C.R., Nogales, C., 1949. Protection des Ports. XVIIth International Navigation Congress, Section II. Communication, pp. 31–80.

Longuet-Higgins, M.S., Stewart, R.W., 1964. Radiation stresses in water waves: a physical discussion, with applications. Deep-Sea Research vol. 11. Pergamon Press, Great Britain, pp. 529–562.

Melby, J.A., Hughes, S.A., 2003. Armor stability based on wave momentum flux. Proceedings of Coastal Structures '03 Conference, American Society of Civil Engineers, New York.

Rienecker, M.M., Fenton, J.D., 1981. A Fourier approximation method for steady water waves. Journal of Fluid Mechanics vol. 104. Cambridge Univ. Press, United Kingdom, pp. 119–137.

Shore Protection Manual, 1984. U.S. Army Engineer Waterways Experiment Station. (4th ed.), U.S. Government Printing Office, Washington, DC.

Smith, S.F., Swan, C., 2002. Extreme two-dimensional water waves: an assessment of potential design solutions. Ocean Engineering vol. 29. Pergamon Press, Great Britain, pp. 387–416.

Sobey, R.J., 1989. Variations on Fourier wave theory. International Journal for Numerical Methods in Fluids vol. 9. John Wiley & Sons, pp. 1453–1467.

Sobey, R.J., 1992. A local Fourier approximation method for irregular wave kinematics. Applied Ocean Research vol. 14. Elsevier Science, The Netherlands, pp. 93–105.

Sobey, R.J., 1998. Nonlinear Wave Theory, Short Course Notes, U.S. Army Engineer Research and Development Center. Coastal and Hydraulics Laboratory, Vicksburg MI. January 1998.

Wiegel, R.L., 1964. Oceanographical Engineering. Prentice Hall, Englewood Cliffs, NJ.

Williams, J.M., 1985. Tables of Progressive Gravity Waves. Pitman, Boston, MA.